JOURNAL OF OPTOELECTRONICS AND ADVANCED MATERIALS, Vol. 11, No. 2, February 2009, p. 114 - 122

Off-axis PLD: A novel technique for plasmonic engineering of silver nanoparticles

C. L.VEENAS, K. M. NISSAMUDEEN, S. L. SMITHA, V. BIJU[a], K.G.GOPCHANDRAN[*]
Department of Optoelectronics, University of Kerala, Thiruvananthapuram-695 581, India
[a]Department of Physics, University of Kerala, Thiruvananthapuram-695 581, India

Silver nanoparticles of different sizes were prepared by implementing pulsed laser deposition technique by varying the laser energy density and deposition time. The synthesized samples are characterized by UV-visible absorption spectra, Mie plot studies, SEM and AFM. By implementing the off-axis PLD technique for a laser energy density of 12 J/cm^2 and ablation time 30 minutes, a sharp SPR band is observed indicating high monodispersity and smaller particle size. The morphology shows nanocrystalline nature of silver particles with well defined boundaries. An attempt has also been made to understand the influence of chloride addition on the plasmonic character of the nanoparticles.

(Received February 15, 2009; accepted February 25, 2009)

Keywords: Silver nanoparticles, Pulsed laser ablation, Surface plasmon resonance

1. Introduction

Nanoparticles of noble metals have recently become the focus of research because of their unique electronic and optical properties, which are different from those of bulk materials [1] and by the widespread uses in ultrafast optical switches, optical tweezers, labels for biomolecules, optical filters, biosensors, surface enhanced spectroscopies, plasmonics, and chemical sensors. The properties of metal nanoparticles are mainly governed by their shape, size, composition, crystallinity and structure [2, 3]. Silver nanoparticles have attracted a great deal of interest due to their promising properties and potential applications in catalysis, chemical analysis, optical and antimicrobial areas, as well as in surface enhanced Raman spectroscopy [4]. The electronic confinement in Ag nanoparticles induces dramatic changes in the optical properties. These changes are caused by surface plasmon resonances (SPRs) that come from the electromagnetic field excitation inside the particles associated with the collective oscillation of the electrons [5]. The oscillation frequency is determined by four factors namely the density of the electrons, the effective electron mass, shape and size of the charge distribution. The field of plasmonics offers several research opportunities including plasmonic chips that function as ultra-low loss optical interconnects, plasmonic circuits and components that can guide light within the ultra compact optically functional devices and super lenses that enable optical imaging with unprecedented resolution. Surface plasmons provide the possibility of localization and the guiding of light in sub wavelength metallic structures and it can be used to construct miniaturized optoelectronic circuits with subwavelength components [6]. There are reports showing the realization of an active plasmonic device by combining thin polymer films containing molecular chromophores with thin silver film [7]. The wavelength of the peak absorption attributed to SPR depends on their particle size, height, shape, particle-to-particle distance and surrounding dielectric medium, the tunable SPR wavelength in the visible and near infrared regions has been achieved by changing these parameters of the metallic nanoparticles [8-12]. Controlling the particle size of the metal nanoparticles is very important due to their size dependent properties [4].

Ag nanoparticles can be deposited by several techniques such as thermal evaporation [13], sputtering [14], ion implantation [15], chemical vapour deposition [16], chemical reduction [17] and pulsed laser deposition (PLD) [18]. In the present investigation Ag nanoparticles were prepared by PLD technique in which both on-axis and off-axis deposition are implemented. Formation of nanoparticles under laser ablation of solids either in gas or in vacuum has been extensively explored during the last decade [19]. PLD is a very convenient technique for nanoparticle preparation, which excites only a small area on the target by the focused laser beam. Even though the laser–target interaction is a very complex process in terms of theoretical understanding, the interest in PLD is growing quickly due to the numerous advantages offered by this method. Unlike other deposition methods, PLD involves a number of controlling parameters such as laser fluence, repetition rate of laser, laser wavelength for the material deposition, target to substrate distance etc [20]. In the present work, silver nanoparticles are deposited by both on-axis and off-axis method by varying the laser fluences. In the off-axis geometry, the substrate is placed perpendicular to the target. By implementing the off-axis PLD technique for a laser energy density of 12 J/cm^2 with an irradiation time of 30 minutes, a sharp SPR band is observed indicating high monodispersity and smaller

particle size. The size of Ag nanoparticles is studied using Mie plot and the morphology using SEM and AFM.

2. Experimental details

2.1 Preparation of silver nanoparticles

Ag nanoparticles were deposited by pulsed laser deposition technique with Ag target using a Q-switched Nd:YAG laser, (Quanta-ray INDI-series, spectra-physics) for a laser energy density of 6 J/cm^2 at 532 nm, having a pulse width of 7 ns with a repetition frequency of 10 HZ. The target was rotated with constant speed to ensure uniform ablation. Fused quartz substrate was kept at a distance of 6.5 cm from the target. In the off-axis geometry, the substrate is horizontal to the normal axis of the target surface and aligned to the centre of the laser spot. The distance between the target and substrate was about 3 cm for the off-axis deposition. Typical experimental set up is shown in Fig. 1.

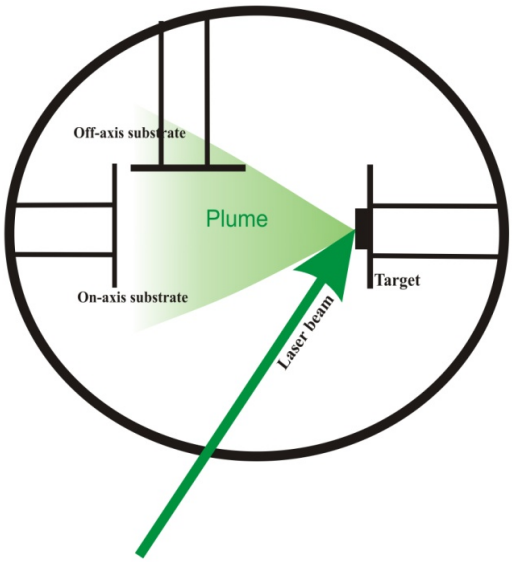

Fig. 1. Schematic representation of experimental set up.

During the ablation of the laser, the chamber was evacuated to a base pressure of 10^{-6} Pa and the ablation was carried out at room temperature for a deposition time of 5 minutes. The effect of laser energy density on the formation of Ag nanoparticles was studied by preparing Ag nanoparticles by varying the laser fluences as 6, 8, 10 and 12 J/cm^2 for an ablation time of 5 minutes by on-axis and off-axis method. The influence of laser ablation time on Ag nanoparticles formation by on-axis and off-axis method can also be studied by varying the ablation time for a laser energy density of 12 J/cm^2. An attempt has also made to study the effect of addition of KCl on the synthesized Ag nanoparticles.

2.2 Instrumentation

The UV-visible spectra were recorded using Jasco V-550 UV-visible spectrophotometer. Size determination of the silver particle is carried out by drawing the Mie plot using the software. The morphology of the particles were investigated by scanning electron microscopy (SEM), using Sirion system and atomic force microscopy (AFM), using Nanoman II, Veeco instrument.

3. Results and discussion

3.1 UV-visible absorption studies

Fig. 2 shows the UV-vis absorption spectra of Ag nanoparticles deposited using on-axis PLD technique by varying laser energy density as 6, 8, 10 and 12 J/cm^2 for an ablation time of five minutes. The absorption band in the visible light region is typical for Ag nanoparticles. The optical absorption spectrum of Ag nanoparticles is dominated by SPR, which shifts towards the blue end or red end depending on the particle size, shape and surrounding medium [21]. The position and number of peaks is related to the size, shape and material of the nanoparticles. Figure 2 reveals that the laser energy density has a strong influence on the formation of Ag nanoparticles. For a laser energy density of 6 J/cm^2, a small peak in the SPR region is observed along with a shoulder peak in the longer wavelength region and the SPR peak in the absorption spectra becomes prominent from a laser energy density of 8 J/cm^2, suggesting that there exists a critical particle size and metal concentration below which the SPR is suppressed [22]. For a laser energy density of 8 J/cm^2 an absorption spectrum with SPR peak wavelength at 433 nm is observed. When the laser energy density is increased to 10 J/cm^2, broadening of SPR band along with a red shift in peak position at around 470 nm was observed. This broadening of SPR is apparently connected with more dispersion in size of metal nanoparticles. The increase in size dispersion may be connected with the possibility of aggregation of nanoparticles [23]. It further red-shifts to 509 nm for a laser energy density of 12 J/cm^2. As the laser energy density increases, the SPR wavelength red shifts, indicating an increase in the particle size [24]. The above shift may be attributed to an increased electromagnetic interaction between the Ag particles with the systematic decrease of surface to volume ratio [25-27]. The presence of SPR in this range is in agreement with the earlier reports [4, 25]. The SEM micrograph of Ag nanoparticles deposited on-axis with minimum required laser energy (8 J/cm^2), for which SPR was observed is shown in figure 3. It exhibits morphology consisting of nanocrystalline nature. Gupta *et al.* [10] have synthesized Ag nanoparticles with thermal evaporation method and by changing substrate temperature, deposition rate and film thickness, the SPR wavelength is tuned from 355 to 1090 nm.

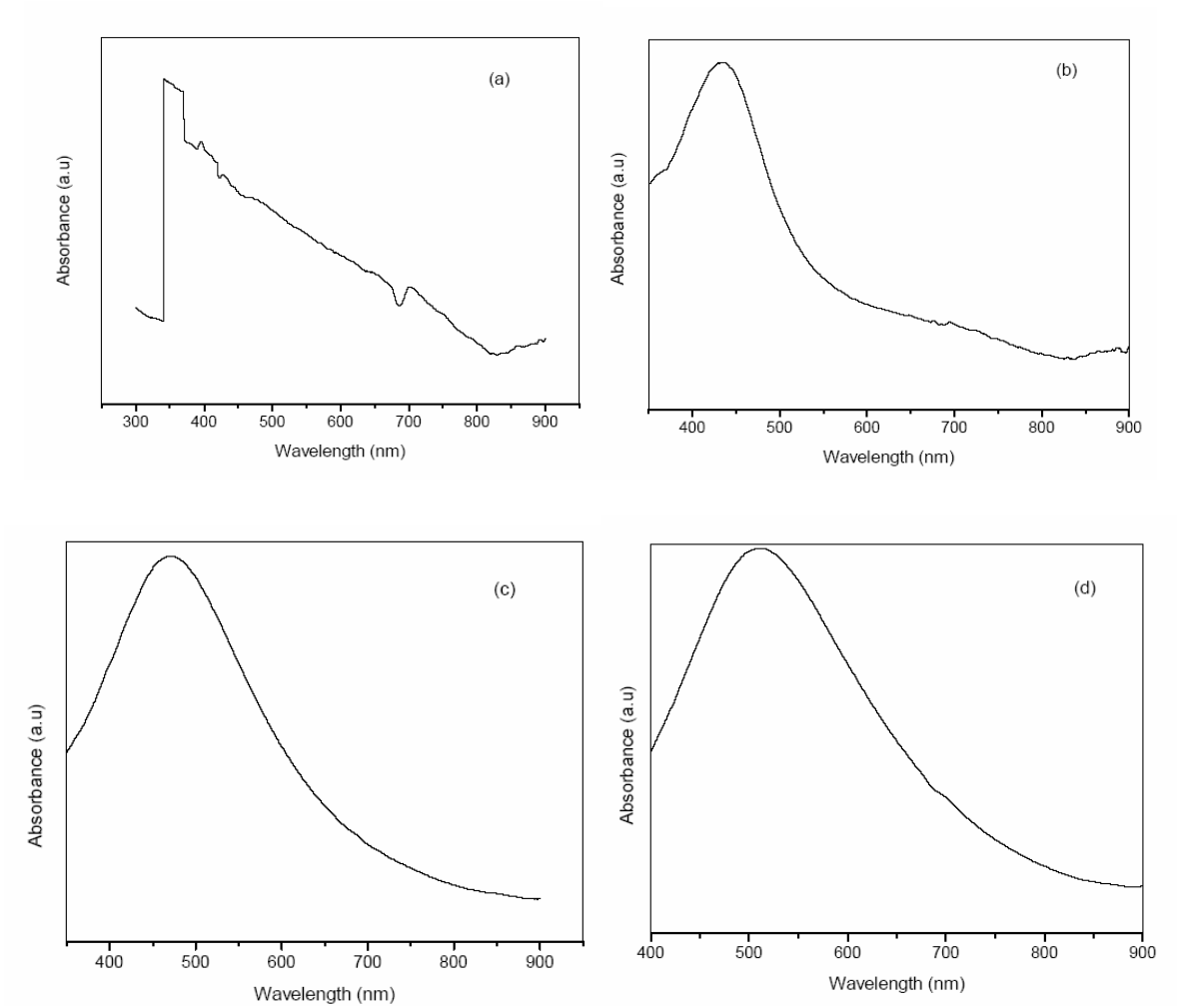

Fig. 2 Absorption spectrum of Ag nanoparticles at different laser energy density by on-axis PLD: (a) 6, (b) 8, (c) 10 and (d) 12 J/cm^2 , for an ablation time of 5 minutes.

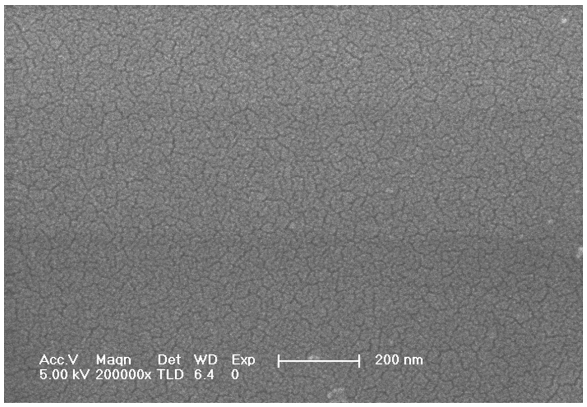

Fig. 3. SEM micrograph of Ag nanoparticles deposited with energy density of 8 J/cm^2 and ablation time 5 minutes by on-axis PLD

Fig. 4 shows the absorption spectrum of Ag nanoparticles deposited by off-axis PLD technique by varying the laser energy density from 6 to 12 J/cm^2 for an ablation time of five minutes. From the figure it can be seen that up to a laser energy density of 10 J/cm^2, a small peak in the SPR region is observed with a shoulder peak in the longer wavelength side which shows a reduction in its width with increase of laser energy. A broad SPR arises for a laser energy density of 12 J/cm^2 which again shows that there exists a threshold value of metal concentration for the formation of SPR [22].

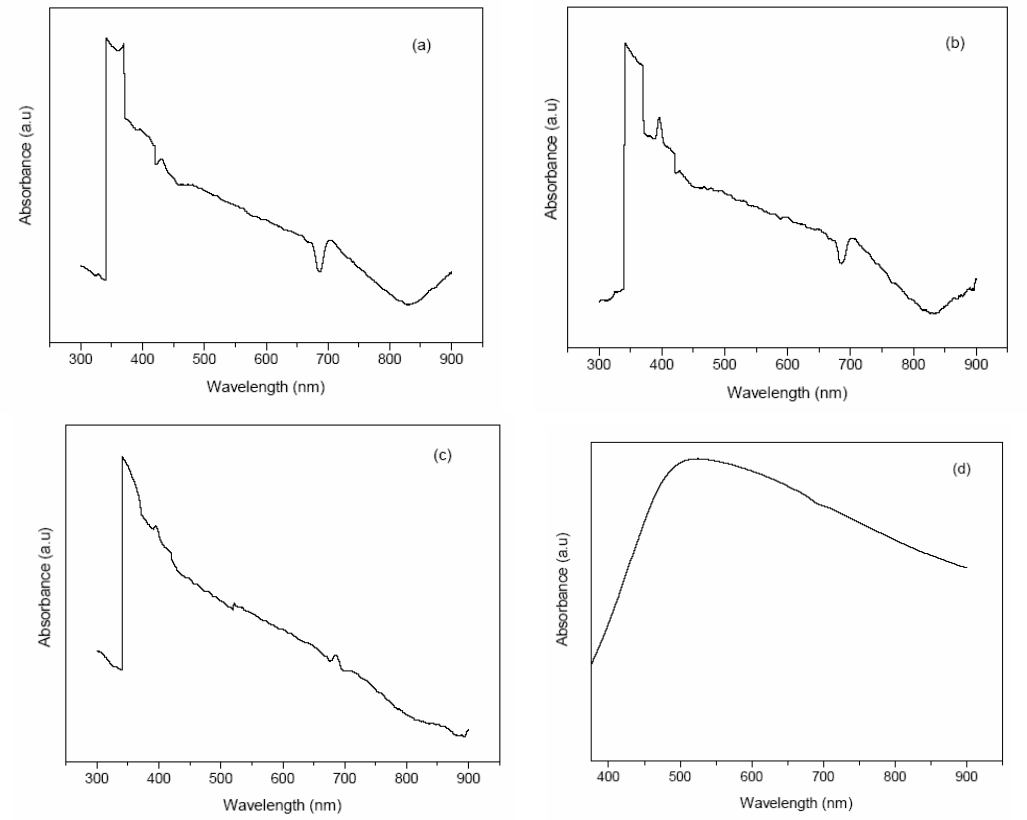

Fig. 4. Absorption spectrum of Ag nanoparticles at different laser energy density by off-axis PLD: (a) 6, (b) 8, (c) 10 and (d) 12 J/cm^2, for an ablation time of 5 minutes.

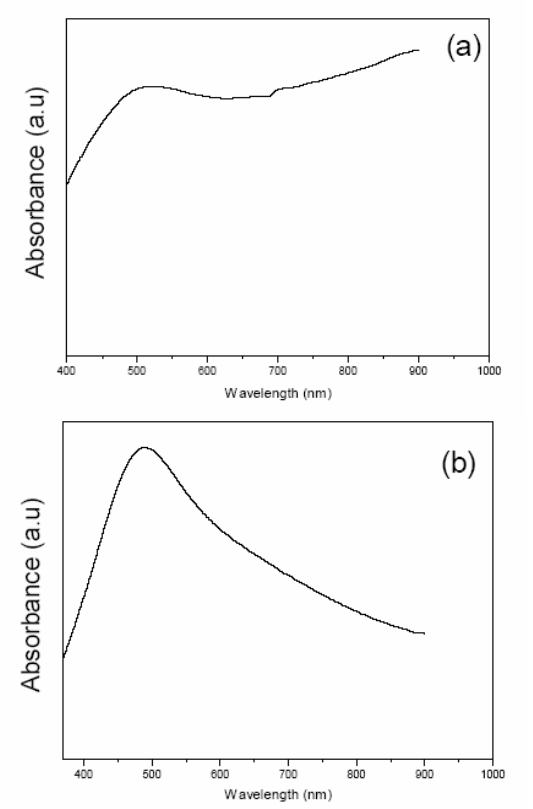

Fig. 5. Absorption spectrum of Ag nanoparticles by on-axis PLD for an ablation time of 30 minutes at a laser energy density of: (a) 8 and (b) 12 J/cm.^{2}

Figs. 5 and 6 shows the absorption spectra of Ag nanoparticles deposited by on-axis and off-axis PLD technique for an energy density of 8 and 12 J/cm^2 ablated for 30 minutes. The absorption spectrum clearly shows a blue-shift in SPR wavelength with increase in laser energy density. This blue-shift was attributed to the reduced spill-out effect of the valence electrons by screening of 4d electron in Ag [28, 29] and is an indication of decrease of particle size.

From Fig. 5 (a) it is clear that for a laser energy density of 8 J/cm^2 , in addition to a single peak at 509 nm corresponding to the transverse oscillation, there arises another peak at 896 nm of higher absorbance due to the longitudinal oscillation which is an indication of formation of rod shaped particle [30]. For a laser energy density of 12 J/cm^2 shown in figure 5 (b), peak at higher wavelength corresponding to longitudinal oscillation disappears completely and only a single peak corresponding to transverse oscillation is seen which can be attributed due to the formation of spherical particles. From figure 6 (a) & (b) it can be seen that for a laser energy density of 8 J/cm^2 a broad spectrum with an SPR at 497 nm is observed and with increase in laser energy density the SPR is blue shifted to 431 nm and the SPR width decreases which is an indication of smaller particle size with high monodispersity [31]. Figure 7 shows the AFM image of Ag nanoparticles deposited with 8 J/cm^2 energy density and ablation time 30 minutes in off-axis method for which SPR was observed with minimum laser energy. Figure 8

and 9 shows the SEM and AFM images of Ag nanoparticles deposited with 12 J/cm^2 ablated for 30 minutes in off-axis. The morphology shows nanocrystalline nature with well defined boundaries. Comparing figure 7 and 9, it can be seen that the thickness increases from 5 nm to 10 nm with increase in laser energy. The reduction in grain size observed in figure 9 is due to increase in thickness of the film. Comparing the sector diagram it can be seen that the roughness of the film increases with laser energy density. The optimized laser energy density of 12 J/cm^2 resulted from the above discussion is used for studying the influence of ablation time on the formation of Ag nanoparticles.

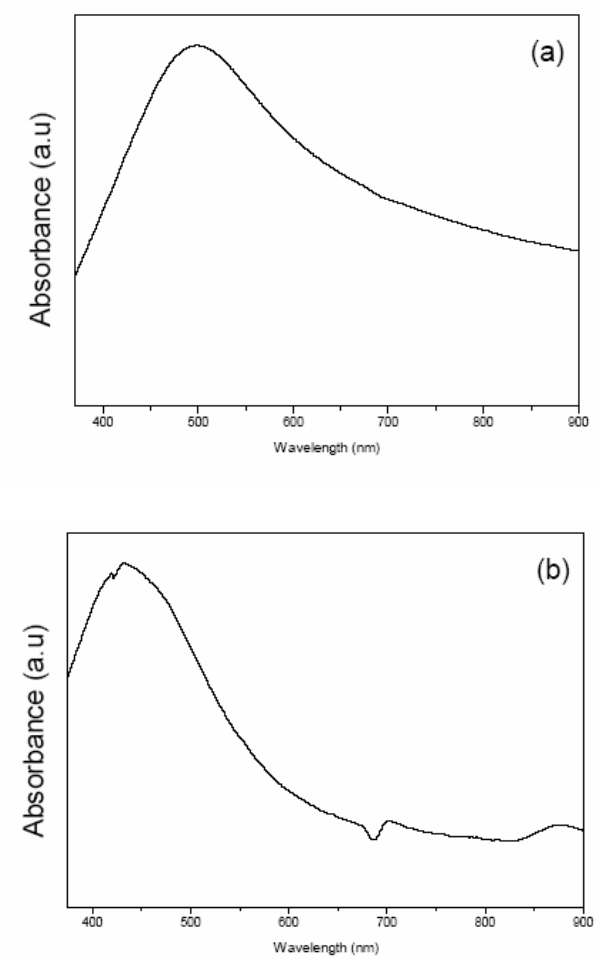

Fig. 6. Absorption spectrum of Ag nanoparticles by off-axis PLD for an ablation time of 30 minutes at a laser energy density of: (a) 8 and (b) 12 J/cm^2.

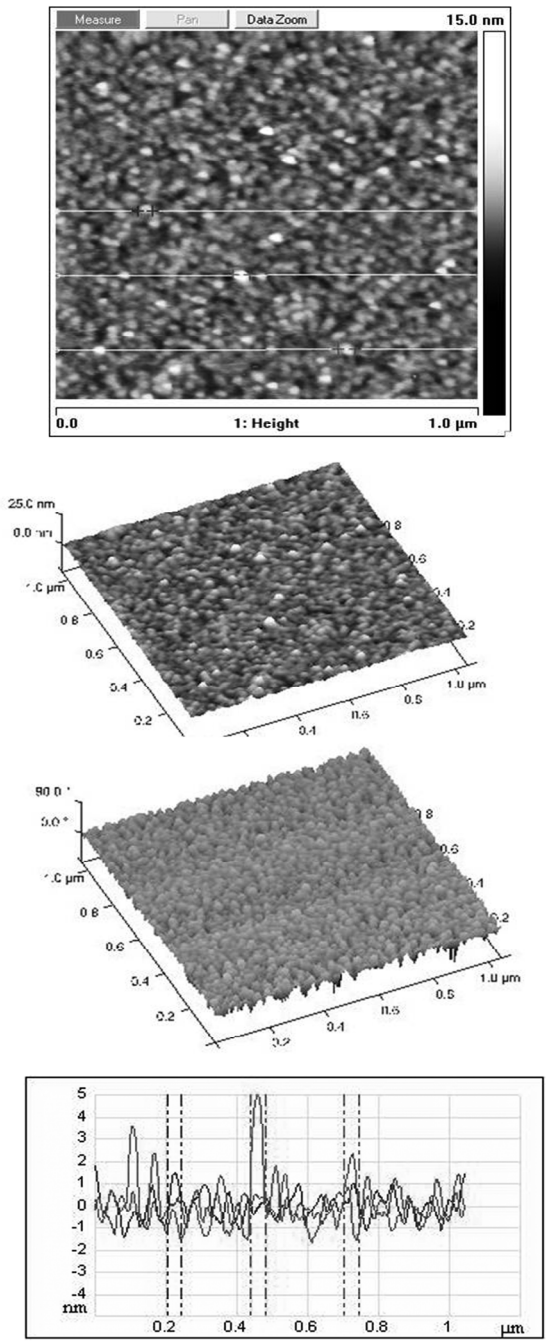

Fig. 7. AFM image of Ag nanoparticles deposited for an ablation time 30 minutes by off-axis PLD with energy density of 8 J/cm^2.

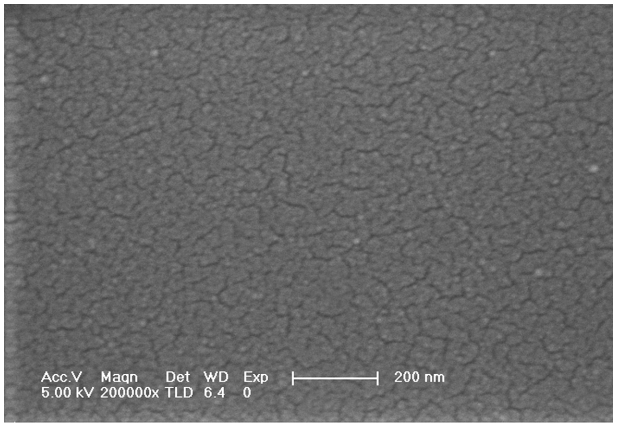

Fig. 8. SEM micrograph of Ag nanoparticles deposited with energy density of 12 J/cm^2 and ablation time 30 min. by off-axis PLD.

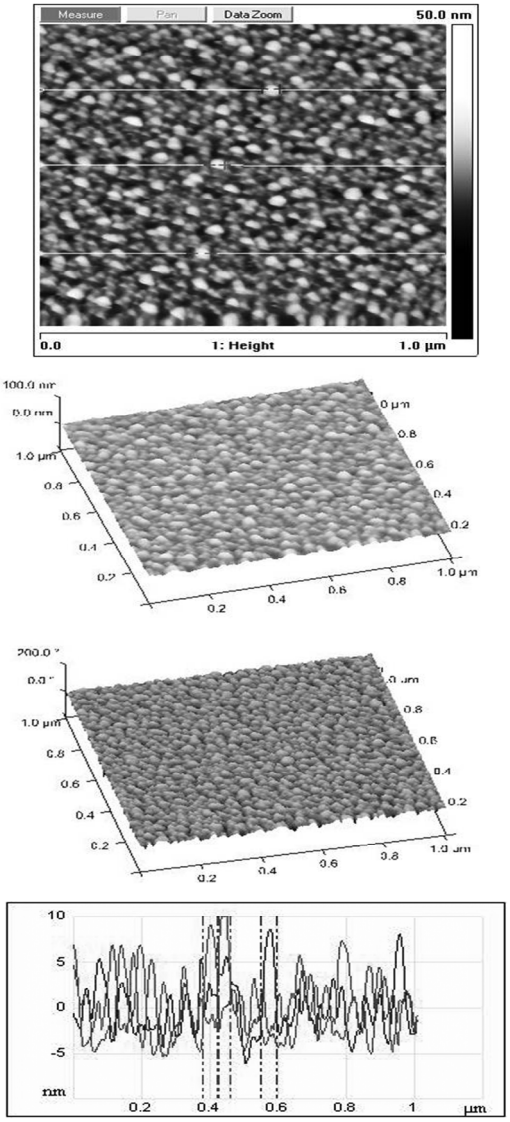

Fig. 9. AFM image of Ag nanoparticles deposited for an ablation time 30 minutes by off-axis PLD with energy density of 12 J/cm^2.

Fig. 10 & 11 shows the absorption spectrum of Ag nanoparticles formed for a laser energy density of 12 J/cm^2 at various ablation time of 2, 5 and 30 minutes by both on-axis and off-axis method. It is evident from figure 10 that the SPR red-shifts from 461 to 509 nm when the irradiation time is increased to 5 minutes and for a time of 30 minutes it blue-shifts to 488 nm. The optical absorbance spectra are dominated by a single absorption peak corresponding to the dipolar interaction between the particles. The dipolar red-shifts due to the strong build up of charges at the gap between the particles [32]. As the ablation time increases, the particle overlaps and due to decoupling the SPR blue-shifts. In the off-axis method shown in figure 11, only a small peak in the SPR region along with a peak in the longer wavelength side is observed for a deposition time of 2 minutes. A prominent SPR arises at 517 nm for a deposition time of 5 minutes and it further blue-shifts and becomes narrower for a time of 30 minutes which is an indication of small and high monodisperse particles. The variation of SPR wavelength with energy density and ablation time by on-axis and off-axis method is given in Table 1.

Table 1. Variation of SPR wavelength with energy density and ablation time by on-axis and off-axis method.

Energy density (J/cm^2)	Deposition time (minutes)	On-axis		Off-axis	
		SPR wavelength (nm)	FWHM (nm)	SPR wavelength (nm)	FWHM (nm)
6	5	-	-	-	-
8	5	433	84	-	-
	30	509	204	497	226
10	5	470	131	-	-
12	2	461	132	-	-
	5	509	140	517	261
	30	488	121	431	97

In order to study the effect of KCl, a 10^{-2}M solution is prepared and the Ag nanoparticles deposited for a laser energy density of 12 J/cm^2 ablated for 30 minutes by off-axis method is allowed to dip for 1, 2 and 3 hours respectively and the corresponding absorption spectrum is shown in Fig. 12.

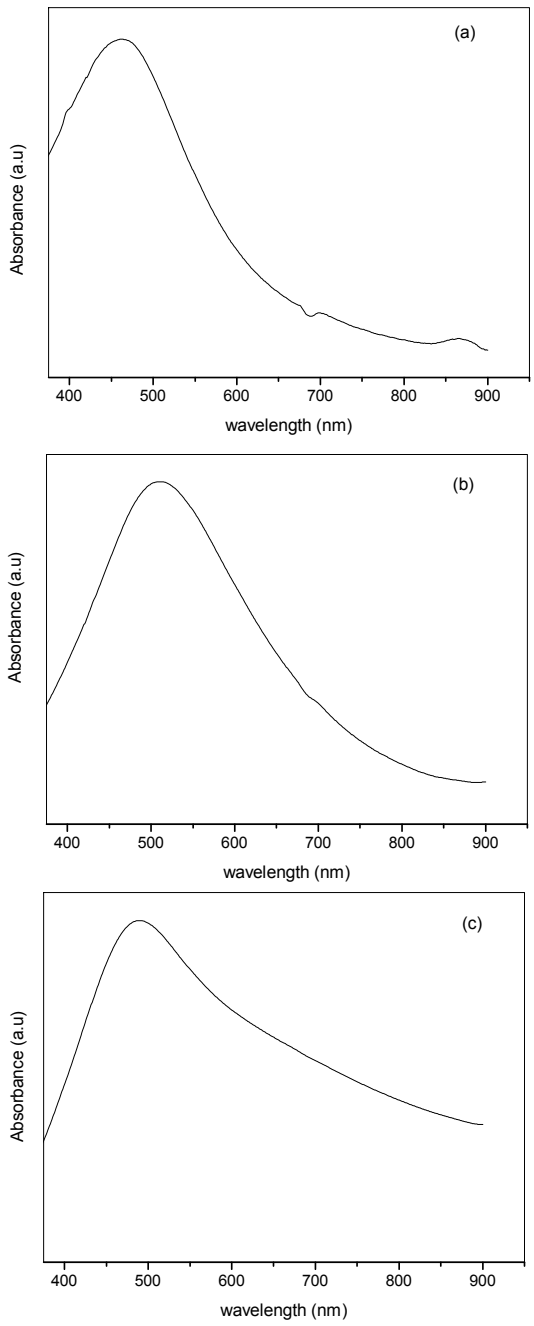

Fig. 10. Absorption spectrum of Ag nanoparticles by on-axis PLD for a laser energy density of 12 J/cm^2 at various ablation time: (a) 2, (b) 5 and (c) 30 minutes.

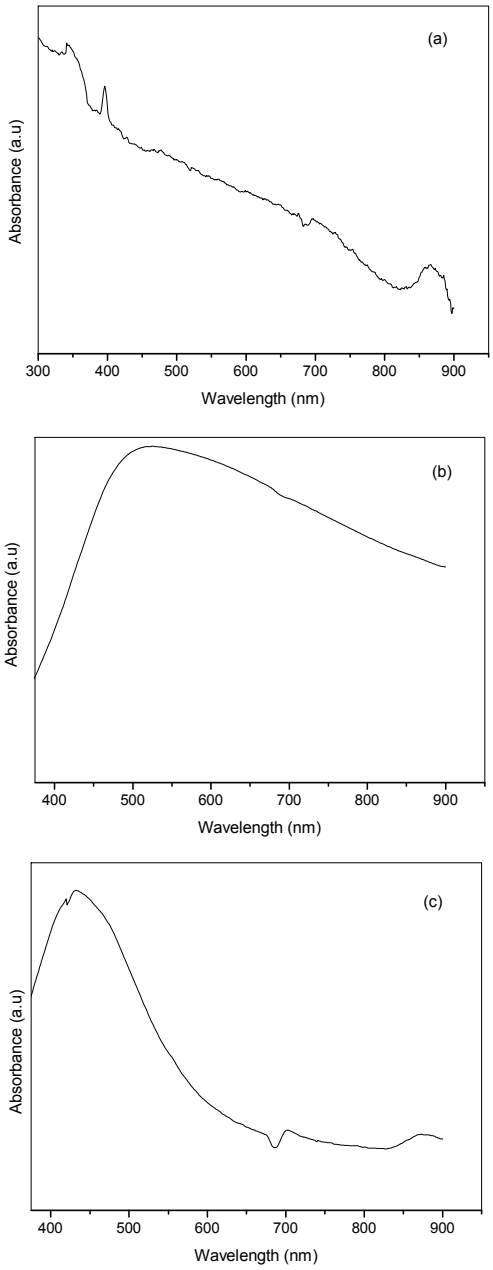

Fig. 11 Absorption spectrum of Ag nanoparticles by off-axis PLD for a laser energy density of 12 J/cm^2 at various ablation times: (a) 2, (b) 5 and (c) 30 min.

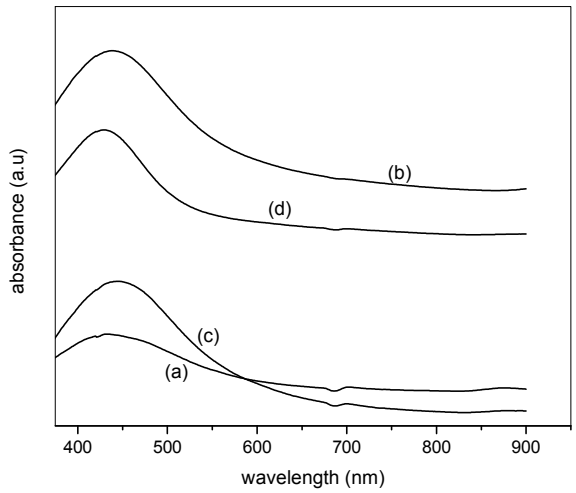

Fig. 12. Absorption spectrum of Ag nanoparticles by off-axis PLD for an energy density of 12 J/cm^2 ablated for 30 minutes treated with KCl at different times: (a) 0, (b) 1, (c) 2 and (d) 3 hours

From the spectrum it is clear that upto 2 hours the SPR peak red-shifts and thereafter a blue-shift occurs. The red-shift can be attributed to the decrease in separation of nanoparticles, which results in increase of average size of nanoparticles [33]. However, there is a limit to the effect of addition of chlorine. Cl^- accelerates the aggregation of the particles. This aggregation is favorable for the observation of intense surface enhanced Raman scattering (SERS) [34, 35].

3.2 Determination of particle size using Mie theory

The classical theory developed by Mie in 1908 predicts that the SPR wavelength should be independent of the particle size at the quasiparticle limit at which the mean particle diameter is smaller than the incident wavelength. Arnold *et al.* [36] built a theoretical curve for the spectral position of SPR absorption maximum as a function of the particle radius. They observed that for silver particles in the R=1-10 nm range the SPR peak position is nearly same and therefore it is difficult to estimate particle size in this region by this approach. In this size regime, the 1/R size dependence of the FWHM of the absorption band is observed and the quasi-static approximation of the Mie theory holds good. Hayakawa *et al* [37] used the relation $R=V_f/\Delta\omega_{1/2}$, where R is the particle radius, V_f is the Fermi velocity of the metal, and $\Delta\omega_{1/2}$ is the FWHM for the absorption band in units of angular frequency, to determine the mean particle radii in this size regime. It is reported that for larger particles, the SPR band is significantly red shifted and subsequently broadened. The broadening of the absorption spectrum is due to the increasingly enhanced free-electron damping in the dielectric constant of silver when the wavelength increases [38]. The 1/R approximation for the particle size estimation is no longer suitable for larger particles. Under such circumstances, a better approximation is achieved by taking into account higher order multipole modes in the Mie relation for the extinction coefficient K (cm^{-1}), which includes both absorption and scattering and when the size of the particles is less than 100 nm, absorption is the dominant attenuation mechanism.

In the present study, the size of the Ag nanoparticles is determined using the Mie software downloaded from the http://www.philiplaven.com/mieplot.htm. Figure 13 shows the absorption spectrum of Ag nanoparticles synthesized for an energy density of 12 J/cm^2 ablated for 30 minutes by off-axis PLD using the data obtained from the Mie plot. A trial and error method was used to make the simulated spectrum to coincide with obtained absorption spectrum. The surface plasmon resonance of the absorption spectrum is obtained at 431 nm. It is the same as that obtained experimentally. Therefore, it can be concluded that the size of the silver particles to be 42 nm in diameter. Similarly the size of the Ag nanoparticles synthesized at various energies by on-axis and off-axis PLD at different ablation time is calculated (not shown). These are in good agreement with the original absorption spectrum.

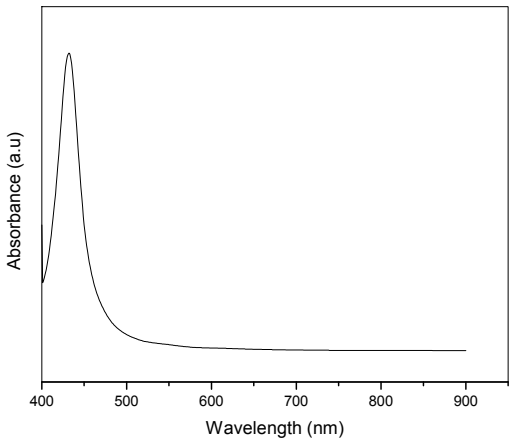

Fig. 13. Absorption spectrum of Ag nanoparticles deposited with energy density of 12 J/cm^2 and ablation time 30 minutes by off-axis PLD obtained from the Mie data.

4. Conclusions

Silver nanoparticles were prepared by pulsed laser deposition technique. The synthesized samples are characterized by UV-visible absorption spectra, Mie plot studies, SEM and AFM. The morphology shows nanocrystalline nature of silver particles. Highly monodisperse particles with a size of 42 nm obtained prepared with a laser energy density of 12 J/cm^2 and 30 minutes ablation time by off-axis geometry. The SPR is found to be sensitive to the addition of chloride ions showing first a red shift and then blue shift with increase

in time after chloride treatment was obtained for particles prepared with a laser energy density of 12 J/cm^2.

References

[1] S. Link, M. B. Mohamed, M. A. El-Sayed, J. Phys. Chem. B. **103**, 3073 (1999).
[2] M. Dankwerts, L Novotny, Phys. Rev. Lett. **98**, 026104 (2007).
[3] J. Roiz, A. Oliver, E. Munoz, L. Rodriquez-Fernandez, J. M. Hernandez, J. C. Cheang- Womg, J. Appl. Phys. **95**, 1783 (2004).
[4] C. Tian, B. Mao, E. Wang, Z. Kang, Y. Song, C. Wang, S. Li, L. Xu, Nanotechnology. **18**, 285607 (2007).
[5] E. Fort, C. Ricolleau, J. Sau-pueyo, Nanolett. **3**, 65 (2003).
[6] E. Ozbay, Science. **311**, 189 (2006).
[7] P. Andrew, W. L. Barnes, Science **306**, 1002 (2004).
[8] R. W. Cohen, G. D. Cody, M. D. Coutts, B. Abeles, Phys.Rev.B**. 8**, 3689 (1973).
[9] T. R. Jensen, M. D. Malinsky, C. L. Haynes, R. P. Van Duyne, J.Phys.Chem.B **104**, 10549 (2000).
[10] R. Gupta, M. J. Dyer, W. A. Weimer, J. Appl.Phys. **92**, 5264 (2002).
[11] G. Xu, M. Tazawa, P. Jin, S. Nakao, K. Yoshimura, Appl. Phys. Lett. **82**, 3811(2003).
[12] S. K. Lim, K. J. Chung, C. K. Kim, D. W. Shin, Y. H. Kim, C. S. Yoon, J.Appl.Phys. **98**, 084309 (2005).
[13] D. K. Lee, Y. S. Kang, ETRI Journal. **26**, 3 (2004).
[14] S. Banerjee, S. Mukherjee, S. Kundu, J. Phys. D: Appl. Phys. **34**, 87 (2001).
[15] V. N. Popok, A. L. Stepanov, V. B. Odzhaeva, J. Appl. Spectr. **72**, 229 (2005).
[16] Y. Yin, Z. Y. Li, Z. Zhong, B. Gates, S. Xia, S. Venkateswaren, J. Mater. Chem. **12**, 522 (2002).
[17] A. Sileikaite, I. Prosycevas, J. Puiso, A. Juraitis, A. Guobiene, Mater. Sci. **12**, 1392 (2006).
[18] J. P. Barnes, A. K. Petford-Long, R. C. Doole, R. Serna, J. Gonzalo, A. S. Garcia, C.N Afonso, D. Hole, Nanotechnology **13**, 465(2002).
[19] S. I. Dolgaev, A. V. Simakin, V. V. Voronov, G. A. Shafeev, F. B. Verduraz, Appl. Surf. Sci. **186**, 546(2002).
[20] V. Resta, J. Siegel, J. Bonse, J. Gonzalo, C. N. Afonso, E. Piscopiello, G V Tenedeloo J. Appl. Phys. **100**, 084311(2006).
[21] K. Patel, S. Kapoor, D. P. Dave, T. Mukherjee, J. Chem. Sci. **117**, 53(2005).
[22] S. K. Mandal, R. K. Roy, A. K. Pal J. Phys. D: Appl. Phys. **35**, 2198(2006).
[23] R. N. Tilki, A. Irajizad, S. N. Mahdavi , J. Appl. Phys. A. **84**, 215(2006).
[24] J. Mock, M. Barbic, D. R. Smith, D. A. Schultz , S. Schultz, J. Chem. Phys. **116**, 6755 (2002).
[25] D. B. Mohan, K .Sreejith, C. S. Sunandana, Appl.Phys B **89**, 59 (2007).
[26] K. Kurihara, C. Rockstuhl, T. Nakano, T. Arai, J. Tominaga, Nanotechnology **16**, 1565 (2005).
[27] T. Donnelly, B .Doggett, J. G. Lunney, Appl.Surf.Sci. **252**, 4445 (2006).
[28] Z. Liebsch, Phys.Rev.B **48**, 11317(1993).
[29] J. Tiggesbaumker, L. Koller, K. H. M. Broer, A. Liebsch, Phys. Rev. A **48**, 1749 (1993).
[30] Paras N. Prasad , Nanophotonics (NewJersey: Wiley Inter Science) (2004).
[31] T. Wenzel, J. Bosbach, A. Goldmann, F. Stietz, F. Trager, Appl. Phys. B **69**, 513(1999).
[32] I. Romero, J. Aizpurua, G. W. Bryant, F. J. G. Abajo, Opt. Soc. Am. **14**, 9988 (2006).
[33] R. J. C. Brown, J. Wang, R .Tantra, R. E. Yardley, M. J. T. Milton, Faraday Dis. **132**, 201 (2006).
[34] D. Philip, G Arudhas, J.Solid State Chem. **114**, 129(1995).
[35] D. Philip, A. John, C. Y. Panicker, H. T. Varghese, Spectrochim. Acta. A **57**, 1561(2001).
[36] G. W. Arnold, J. A. Borders, J. Appl. Phys **48**, 1488(1977).
[37] T. Hayakawa, S. T. Selven, M. Nogami, J. Non-Cryst. Solids. **259**, 16 (1999).
[38] G. Bader, P. V. Ashrit, F. E. Girouard, V. V. Truong , J. Appl. Phys. **68**, 1820 (1990).

*Corresponding author: gopchandran@yahoo.com